Using SIR Modeling to Understand the Relationship Between Pathogens and Population Dynamics

Taylor Beaman[1], Carter Hall[1], Molly McDermott[1], Sam Orenstein[1]

[1] Department of Biology, University of North Carolina at Chapel Hill

---

1 Abstract

In a world recently held captive by the coronavirus (COVID-19) pandemic, an understanding of the faculties through which viruses propagate their existence is critical. Fortunately, the field of epidemiology has, for decades, dedicated itself to quantifying the effects of pandemics and epidemics in efforts to better advise public policymakers and average citizens as they live through unprecedented times.

This report looks to employ biological and statistical techniques to characterize pathogenic behavior across a myriad of scenarios. The topics discussed represent risks to the health of humans, namely the possibility of reinfection and the efficacy of vaccinations. Such analysis is achieved through temporal simulations of modified SIR models (Allen, 1994), as well as a spatiotemporal Monte-Carlo simulation that invokes principles of stochasticity to mimic desired population dynamics.

Key Words: epidemiology, SIR Modeling, pathogen, population dynamics, Monte-Carlo simulation

2 Introduction

The inevitable — and accelerating — emergence of new infectious diseases means that it is critical to understand how pathogens spread through a population. Predicting this behavior allows appropriate actions to be taken to mitigate the spread, produce effective vaccines, and understand how future strains prolong outbreaks. This paper intends to answer questions about how space and population density, as well as vaccines, affect the duration and trajectory of an arbitrary infectious outbreak. This problem is of incredible biological significance in the midst of the COVID-19 pandemic: as vaccines are developed and new coronavirus variants emerge, predictions of the trajectory of the pandemic, spread of the virus, and the effects of the virus change rapidly. Some factors that are of importance to track in the modeling of infectious disease include transmissibility, vaccine efficacy, susceptibility to reinfection, and spatial dynamics in the population. The models behind this paper include these features as either user-defined parameters or stochastic quantities.

Social interactions have significant implications in the spread of a pathogen through the population. A suggested mitigation tactic in the response to viral

spread, as seen during the Covid-19 pandemic, is limiting close contact outside predetermined social "bubbles" and social distancing from everyone else. In this study, the impact of space between members of the population is considered a significant factor in the continuation or ending of a pandemic.

Whether and to what degree distance affects the transmission of disease can inform whether social distancing is an appropriate mitigation tactic to implement during a pandemic. Spatial interactions matter more for places of higher population density. For example, dense urban environments will have far more random interactions between members of the population that can result in transmission; on the other hand, rural and other low-density environments may be more socially distanced already.

Moreover, while perfect social distancing could bring even the most transmissible illness to an end, the mitigation tactic is not without disadvantages. Students no longer attending in-person school learn less, and adults without opportunities to work remotely earn less, exacerbating pre-existing inequalities and indirectly worsening health outcomes. More directly affecting health outcomes is reduced social interaction, which partially explains worsening mental health (Czeisler et al., 2020) and an uptick in domestic violence (Nikos-Rose, 2021). All in all, the consequences of and backlash to imposing social distancing measures may outweigh the putative benefits. Therefore, public health authorities must weigh the costs and benefits of imposing social distancing measures, and models, such as this one, may inform their decision-making. Vaccination is another crucial element for stopping outbreaks and ending pandemics. Other public health measures, such as social distancing or masking, may decrease case numbers, but mass vaccination of a population against infectious disease tends to be most impactful in ending outbreaks long-term by providing individuals with adaptive immunity against the pathogen. For example, polio vaccines have kept the poliovirus completely at bay in the United States for over 40 years now, and vaccines against the flu each year protect against enormous outbreaks (Little, 2020). Vaccines can vary in efficacy against their respective pathogens, especially with new mutations; however, in concert with immunity from previous infections, vaccines of varying efficacies can still lead to herd immunity in a population.

Transmissibility may change significantly over the course of a pandemic with new viral strains, changing symptoms, and vaccination. These constantly changing values are crucial for implementing successful mitigation tactics, such as social distancing. Transmissibility can be modeled by combining the distance between any two individuals and their likelihood of coming in contact. Pathogens can be spread in various ways, including through contact with skin, bodily fluids, airborne particles, feces, or surfaces touched by an infected person, all of which are assumed to be possibilities in SIR mathematical modeling of the disease.

Susceptibility after infection is another important parameter when modeling infectious diseases. Some infectious diseases, such as measles, provide nearly lasting resistance to reinfection (Griffin, 2021). Such diseases' spread may diminish more quickly than those which do not yield long-term immunity. Reinfection can significantly prolong the length of a pandemic, especially when immunity

after infection only lasts for a short period or is nonexistent.

Mathematically modeling infectious disease spread provides incredible insight into how the virus of interest will continue to act based on the nature of the disease and on the parameters governing the model population. This technique is used in this paper with variations of an SIR model and Monte-Carlo simulations to show how an arbitrary viral infection moves through a population before and after vaccines are present. The role of spatial interactions are considered as a potential significant factor of viral spread. These factors are considered to address whether vaccines and social distancing can significantly shorten the length of a pandemic, assuming no other significant changes in the population occur.

3 The Model(s)

This study investigates the spread of a viral pathogen in a population. It is assumed this is a nonfatal infection, as no death rate is included in the model. The analyses apply a modified Susceptible-Infected-Recovered (SIR) model and SIR model with vaccination (SIRV) with Monte-Carlo spatial simulations to three different population density scenarios with and without vaccination.

All models maintain certain assumptions. First, no explicit assumption is made as to the period between two infections. The proportions of individuals subject to reinfection is small, so a significant period of time between infections is assumed. Second, vaccine efficacy is assumed to be constant: while vaccine efficacy against most pathogens tends to wane over time, this decrease in effectiveness is assumed to be negligible. In the model, vaccinated individuals remain in the vaccinated class or infected class but never return to the susceptible class. Keeping vaccine efficacy constant allows the analyses to focus strictly on the effects of spatial interactions with and without vaccines.

3.1 SIR as System of Equations

The Susceptible-Infected-Recovered (SIR) model in Figure 1 is represented by the system of equations in Equations (1a) - (1d), defined below.

$$S_{t+1} = S_t - fS_tI_t \tag{1a}$$
$$I_{t+1} = (1 + fS_t - r)I_t + CR_t \tag{1b}$$
$$R_{t+1} = R_t(1 - C) + rI_t \tag{1c}$$
$$C \sim \mathcal{U}(0, 0.1) \tag{1d}$$

The number of individuals in the susceptible population at time = t+1 is equivalent to the number of susceptible individuals at time t, minus the number of susceptible individuals at time t that become infected based on f, which is a chosen parameter representing the proportion of susceptible individuals at time t that become infected at time $t+1$. The number of individuals in the infected population at time $t+1$ is a function of the number of susceptible individuals time t that become infected by the infection parameter, f, minus the number of infected individuals at t that recover by the chosen recovery rate, r, plus those

that become reinfected from the recovered population at a random reinfection rate, c. The number of individuals in the recovered population at time *t+1* is represented by the number of individuals recovered at time t minus those that become reinfected by the random reinfection rate, c, plus those from the infected population at time t that recover by the recovery rate, r.

3.2 SIRV as System of Equations

In the Susceptible-Infected-Recovered-Vaccinated (SIRV) model, as shown in Equations (2a) - (2e), a fourth equation is added to the system to represent the number of individuals who are vaccinated in the population. The vaccinated population at time *t+1* is represented by the rate of vaccination, b, amongst the susceptible population minus those in the vaccinated population at time t that become reinfected by the random reinfection rate, c. Additional terms are added to each of the susceptible, infected, and recovered population equations. Those vaccinated at a vaccination rate, b, are removed from the susceptible population. Those that become reinfected by a rate of c from the vaccinated population are added to the infected population.

$$S_{t+1} = S_t - fS_tI_t - bS_t \tag{2a}$$
$$I_{t+1} = (1 + fS_t - r)I_t + C(R_t + V_t) \tag{2b}$$
$$R_{t+1} = (1 - C)R_t + rI_t \tag{2c}$$
$$V_{t+1} = (1 - C)V_t + bS_t \tag{2d}$$
$$C \sim \mathcal{U}(0, 0.025) \tag{2e}$$

3.3 Monte-Carlo Simulation: General Steps and Purpose

The SIR and SIRV models provide a basis for how to analyze the data produced by the spatiotemporal models that the Monte-Carlo simulations produce. These simulations are used to randomly move individuals spatially after which infection transmission is determined by whether a susceptible individual is within a distance threshold with an infected individual. At time t=0, N individuals are uniformly placed on a grid of decided size, which varies to represent an average population density. While each model representing urban, suburban, and rural environments will start with the same population size, they will vary in habitat size in order to represent different population densities. The following procedure highlights the general framework of a Monte-Carlo simulation for this category of population dynamics, explained further in psuedocode in Algorithm A:

1. Place N individuals uniformly at random on a grid.
2. According to initial value parameters, mark appropriate counts of individuals for each class of the model.
3. For each iteration:
    - Determine if each individual moves using a Bernoulli trial.
    - If an individual moves, sample amounts from separate Normal distributions representing the amount moved in each coordinate direction.

- Compute a distance matrix of the Euclidean distances between each pair of individuals.
- For each pair of individuals, determine if an infection, or reinfection, can occur. If so, model the appropriate type of infection with a Poisson distribution.
- For each individual, sample a Poisson distribution to determine vaccination or recovery status.
- Count the individuals belonging to each class of the model.

4 Results

4.1 SIR and SIRV System of Equations

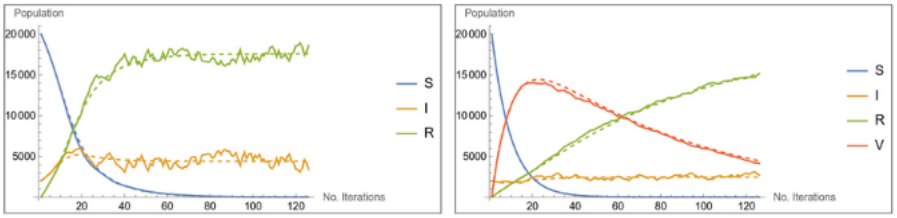

Figure 1: Modeling SIRV Dynamics with Reinfection via Monte-Carlo simulations. Dashed curves represent individual simulations of the Monte-Carlo algorithm (see Appendix A, Algorithm 2), whereas solid curves represent average performances of the algorithm. From left to right, the simulations depict representative population dynamics in urban, suburban, and rural areas, respectively. Each area was determined by the change of expected initial population-density, calculated as $\frac{N}{\text{length}}^2$, where length = ymax − ymin = xmax − xmin. Each individual simulation was conducted over $N_{\text{iter}} = 30$ iterations, and the average was computed from $N_{\text{runs}} = 5$ simulations. The y-axis ranges from 0 to 22000 individuals, and the x-axis ranges from 0 to 125 iterations.

The SIR and SIRV models give baselines for how a viral infection may interact in the population, with and without vaccines, and a result to juxtapose with the performance of their Monte-Carlo counterparts. As can be seen in the SIR and SIRV Models, with reinfection a possibility (Figure 1), the population remains largely recovered from the pathogen, and as the number of susceptible individuals approaches zero, the population is entirely infected at some point by the virus. In the SIRV model, there is a peak of vaccination early in the simulation that wanes over time, given reinfections that occur. The parameters are listed as follows: (SIR) $S_{t=0} = 20000, I_{t=0} = 2000, R_{t=0} = 0, f = 1.5 \cdot 10^{-5}, r = 0.2, c = 0.05$ (when used), (SIRV) $S_{t=0} = 20000, I_{t=0} = 2000, R_{t=0} = V_{t=0} = 0, f = 0.3 \cdot 10^{-5}, r = 0.1, c = 0.0125$ (when used), $b = 0.1$. Both the stochastic (solid line) and deterministic (dashed line) representation of these population dynamics are shown to reflect this trend.

4.2 SIR Monte-Carlo Simulation

The Monte-Carlo simulations consider how spatial interactions within the population affect transmission of the disease. Figure 2, below, shows the resultant infection dynamics in the population in three different population density scenarios without vaccination. The left-most figure represents an urban environment with a high population density. There is an early peak in infection to about 600 individuals, and the susceptible population falls to zero as all members of the population become infected during the 30 time iterations.

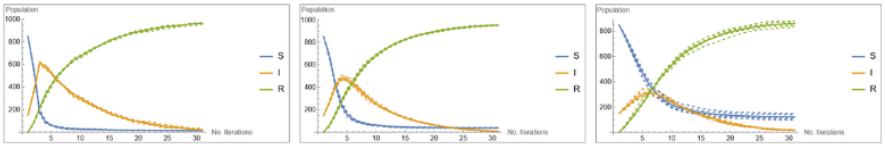

Figure 2: Modeling SIR Dynamics with Reinfection via Monte- Carlo simulations. Dashed curves represent individual simulations of the Monte-Carlo algorithm (see Appendix A, Algorithm 1), whereas solid curves represent average performances of the algorithm. From left to right, the simulations depict example population dynamics in urban, suburban, and rural areas, respectively. Each area was determined by the change of expected initial population density, calculated as $\frac{N}{\text{length}}^2$, where length = ymax − ymin = xmax − xmin. Each individual simulation was conducted over $N_{\text{iter}} = 125$ iterations, and the average was computed from $N_{\text{runs}} = 5$ simulations. The y-axis ranges from 0 to 1000 individuals, and the x-axis ranges from 0 to 30 iterations.

The right-most graph in Figure 2 represents a rural environment with a low population density. Here, the susceptible population does not reach zero over the same timeframe, and the peak in infections is comparatively smaller at about 300. The middle graph represents a suburban environment with an intermediate population density. The infection peak is also between the other two graphs at about 450, and the susceptible population becomes very small by the end of the simulation, though it does not reach zero. The entire population did not become infected over the course of the simulation as in the urban environment, but a larger proportion became infected than in the rural environment. The parameters of the SIR Monte-Carlo simulations are as follows: $N = 1000, S_{t=0} = 850, I_{t=0} = 150, R_{t=0} = 0, d_{\text{thresh}} = 1, \text{inf}_{\text{thresh}} = 2, \textit{permImmunity} = \text{False}, r_{inf} = 0.25, \text{rec}_{\text{thresh}} = 2, \lambda_{\text{rec}} = 3, N_{\text{iter}} = 30, N_{\text{runs}} = 5$.

It is important to note the arbitrarily chosen $d_{\text{thresh}}, \text{inf}_{\text{thresh}}, \lambda_{\text{rec}}$, and $\text{rec}_{\text{thresh}}$ parameters – through implementation of infection and recovery processes with Poisson distributions, the probability of infection for any one susceptible individual coming in contact with an infected person falls approximately in the interval $(0, 0.08)$ (note the use of $p_{\min}$ and $p_{\max}$ to reflect the bounds of these intervals), as depicted below in Equation 3 (note $X \sim \text{Pois}(\lambda)$ is an arbitrary random variable that represents the decisions made for infection, recovery, and vaccination as in Appendix A). Likewise, the probability of recovery for an infected individual falls approximately in the interval $(0, 0.58)$. Such values are derived from the recognition that the argument to the distribution modeling infection, λ_{inf},

approaches zero when two individuals' distance apart nears the d_{thresh} value, and conversely approaches said threshold as the distance approaches zero; a similar process was used when considering parameters for recovery.

$$(p_{\min}, p_{\max}) = (lim_{\lambda \to 0} P(X > \inf_{\text{thresh}}), lim_{\lambda \to d_{\text{thresh}}} P(X > \inf_{\text{thresh}})) \quad (3)$$

4.3 SIRV Monte-Carlo Simulation

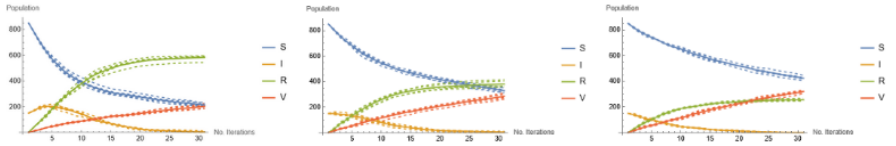

Figure 3: Modeling SIRV Dynamics with Reinfection via Monte- Carlo simulations. Dashed curves represent individual simulations of the Monte Carlo algorithm (see Appendix A, Algorithm 2), whereas solid curves represent average performances of the algorithm. From left to right, the simulations depict representative population dynamics in urban, suburban, and rural areas, respectively. Each area was determined by the change of expected initial population-density, calculated as $\frac{N}{\text{length}}^2$, where length = ymax − ymin = xmax − xmin. Each individual simulation was conducted over $N_{\text{iter}} = 30$ iterations, and the average was computed from $N_{\text{runs}} = 5$ simulations. The y-axis ranges from 0 to 1000 individuals, and the x-axis ranges from 0 to 30 iterations.

When vaccination is considered in these spatiotemporal models of pathogen transmission, the spread of the disease is mitigated by immunization in all three population densities. In the urban representation with the highest population density in the left-most graph of Figure 3, there are more infections than the other environments with a peak of over 200, but this is about a third of the peak number of infections in the same environment with no vaccination. Infection numbers reach zero after some time as vaccination increases. The susceptible population decreases over time due to infection and vaccination, but it remains well above zero, indicating that a large proportion of the population never became infected.

In the suburban (intermediate population density) representation, as shown in the middle graph of Figure 3, there is no peak of infection after the initial infected proportion of the population; the number of infected individuals in each time interval decreases with each interval until it reaches zero. With vaccination, the suburban environment has far fewer total infections compared to the same environment without vaccination, represented by a consistently high number of susceptible individuals and fewer number of infections per time iteration. With equivalent vaccination rates, there are fewer infections in the less dense suburban environment than in the urban environment.

The rural environment with vaccination, shown in the right-most graph of Figure 3, shows even less infection, with infection numbers dropping to zero very quickly. The susceptible population remains high and the recovered population

remains low with the same vaccination rate as the suburban and urban environments, indicating this population had the smallest proportion of infections in the population. Compared to the same environment without vaccination, there was less infection as well.
The SIRV Monte-Carlo simulation parameters are as follows: $N = 1000, S_{t=0} = 850, I_{t=0} = 150, R_{t=0} = 0, V_{t=0} = 0, d_{\text{thresh}} = 1, \text{inf}_{\text{thresh}} = 2, \textit{permImmunity} = \text{False}, r_{inf} = 0.15, \text{rec}_{\text{thresh}} = 2, \lambda_{\text{rec}} = 3, r_{\text{inf},V} = 0.1, \text{vac}_{\text{thresh}} = 5, \lambda_{vac} = 2, N_{\text{iter}} = 30, N_{\text{runs}} = 5$.

5 Discussion

When looking at the traditional SIR model with the possibility of reinfection, we see that both the populations with and without vaccinations are able to successfully reduce their susceptible population to zero. However, it took more iterations for the unvaccinated population to reach this equilibrium. This implies that with the aid of vaccinations, communities not only fight off pathogens at a much higher rate, but also prevent future pandemics. While protection due to vaccinations is biologically realistic, our model introduced vaccinations at the same time as initial infections. In reality, vaccinations cannot be introduced until the pathogen is identified and effective vaccinations are researched prior to distribution.

Once we successfully modeled a viral outbreak using SIR and SIRV models, we overlaid these models with a spatial model to assess how varying population densities and social distancing affected transmission of the illness. We first assessed this spatial model without vaccinations present in urban, suburban, and rural communities. It should be noted that starting population densities differed, and as individuals moved through each simulation, the population density varied depending on the random movement.

Urban models contained high population densities, which resulted in exponential growth and later rapid decay in the number of susceptible individuals before reaching zero at equilibrium. On the contrary, the rural model contained a low population density, which resulted in a small initial spike of infected individuals and an equilibrium with susceptible individuals greater than zero. This means that there was a proportion of the population that was never infected by the pathogen due to the decrease in population density. With an intermediate value for population density in the suburban model, the equilibrium of susceptible individuals is zero, meaning all individuals were infected. Though we predicted communities with higher population densities to become infected more quickly, we did not anticipate such a large proportion of individuals to be susceptible after several iterations in populations with lower population densities. Social distancing was implicitly modeled through the differing population density parameters; we find that populations with increased social distancing (low population density) were able to overcome the pandemic more quickly while also having individuals who were never infected with the pathogen. From a biological standpoint, this reflects that low population density — whether inherently present or imposed in the form of social distancing — is effective in reducing both pandemic severity and length.

Next, we reran the Monte Carlo simulations with the same three population densities but introduced vaccination parameters. Similar to the previous simulation, communities with more social distancing and/or lower population densities had a smaller initial spike in infected individuals compared to the other communities, which quickly reached an equilibrium of zero. However, with the aid of vaccinations, all communities successfully overcome the pandemic while preventing several individuals from getting infected. This is represented by the large equilibrium of susceptible individuals across all three simulations, though the number of susceptible individuals at equilibrium is largest in the rural model. Therefore, with the aid of both vaccinations and social distancing, we can end a pandemic while also providing protection for future outbreaks of that virus. Our results align with our expectations, given the success of vaccinations and social distancing in the current Covid-19 pandemic. However, we were surprised at the large impact of social distancing alone when a pathogen is introduced with the potential for reinfection.

To build on this model, we would consider adding a parameter to represent death rate. This parameter should include both deaths due to the virus and unrelated causes. If added, the resulting population dynamic would be more realistic. Our model also did not address the issue of viral mutations and how these may result in declines in vaccine efficacy. Similarly, we assumed constant vaccine efficacy over time, though immunity likely wanes, exemplified by the fact that common vaccines require several doses to maintain protection.

Finally, our model could have been more biologically realistic if the individuals were not presumed to be identical. Because all individuals were subjected to the same stochasticity at every point in the Monte Carlo simulation, they were assumed to be identically risk-tolerant: equally likely to move around the area, contract and transmit illness, and get vaccinated. This assumption applied both within each area and between areas. Within areas, some individuals, such as elderly adults and immunocompromised people, are more likely to contract viral infections and experience worse outcomes, which may motivate them to comply with social distancing and vaccination. Age, gender, health status, and political affiliation explain individuals' risk tolerance and compliance with social distancing. Our model could have approximated this complexity by assigning some individuals to a low movement, high vaccination class and others to high movement, low vaccination class.

Different areas may also have different cultural attitudes towards complying with public health measures and vaccination, especially given how vaccination status, political polarization, and population density are correlated (Hamel et al., 2021). Instead of assuming the only difference between rural, suburban, and urban areas is the average distance between individuals, we could have better simulated real-world conditions by modifying each area's movement and vaccination parameters.

6 Literature Cited

Allen, L. 1994. Some Discrete-Time SI, SIR, and SIS Epidemic Models. Retrieved from 10.1016/0025-5564(94)90025-6

Czeisler MÉ , Lane RI, Petrosky E, et al. 2020. Mental Health, Substance Use, and Suicidal Ideation During the COVID-19 Pandemic — United States, June 24–30, 2020. MMWR Morb Mortal Wkly Rep 2020;69:1049–1057. Retrieved from http://dx.doi.org/10.15585/mmwr.mm6932a1externalicon.

Hamel, L, et al. 2021. KFF COVID-19 Vaccine Monitor: September 2021. Retrieved from https://www.kff.org/coronavirus-covid-19/poll-finding/kff-covid-19-vaccine-monitor-september-2021/

Griffin, D.E. 2021. Measles Immunity and Immunosuppression. Current Opinion in Virology. 46:9-14. Retrieved from https://doi.org/10.1016/j.coviro.2020.08.002.

IBM Cloud Education. 2020. What is Monte Carlo simulation? Retrieved from https://www.ibm.com/cloud/learn/monte-carlo-simulation

Little, B. 2020. 4 Diseases You've Probably Forgotten About Because of Vaccines. History. Retrieved from https://www.history.com/news/vaccines-diseases-forgotten.

Nikos-Rose, K. 2021. COVID-19 Isolation Linked to Increased Domestic Violence, Researchers Suggest. Financial Stress Contributes. Retrieved from https://www.ucdavis.edu/curiosity/news/ covid-19-isolation-linked-increased-domestic-violence-researchers-suggest

7 Appendix A: Monte-Carlo Simulations

The following pages outline the implementation of the two Monte Carlo simulations in psuedocode. The simulations were performed in Wolfram Mathematica 13.0 Student Edition.

Algorithm 1 Simulation for Basic SIR Model

Require: $S_t + I_t + R_t = N \; \forall t \wedge N, T \in \mathbb{Z}_+$

$x_1, x_2, ..., x_N \sim \mathcal{U}(\text{xmin}, \text{xmax}); y_1, y_2, ..., y_N \sim \mathcal{U}(\text{ymin}, \text{ymax})$

$$s_1, s_2, ..., s_N := \begin{cases} S & 1 \leq i \leq S_{t=0} \\ I & S_{t=0} < i \leq S_{t=0} + I_{t=0} \\ R & \text{otherwise} \end{cases}$$

Res $\leftarrow [0]^{N \times 3}$
t $= 1$
while $t \leq T$ **do**
  $m_1, m_2, ..., m_N \sim Bern(p_{\text{move}})$
  for $i = 1, i \leq N$ **do**
    if m_i **then**
      $x_i \leftarrow x_i + \mathcal{N}(0, 1)$
      $y_i \leftarrow y_i + \mathcal{N}(0, 1)$
    end if
  end for
  D $\leftarrow [0]^{N \times N}$
  for $i \in [1, N] \cap \mathbb{Z}$ **do**
    for $j \in [1, N] \cap \mathbb{Z}$ **do**
      $D_{i,j} = \sqrt{(x_i - x_j)^2 + (y_i - y_j)^2}$
    end for
  end for
  for $i \in [1, N] \cap \mathbb{Z}$ **do**
    for $j \in [i + 1, N] \cap \mathbb{Z}$ **do**
      if $(s_i = I \vee s_j = I) \wedge D_{i,j} < d_{\text{thresh}}$ **then**
        $\lambda_{inf} = |D_{i,j} - d_{\text{thresh}}|$
      end if
      infect $\leftarrow Pois(\lambda_{inf})$
      if permanent immunity **then**
        infect $\leftarrow 0$
      else if $s_i = R \vee s_j = R$ **then**
        $\lambda \leftarrow r_{\text{inf}} * \lambda_{inf}$
        infect $\leftarrow Pois(\lambda_{inf})$
      end if
      if infect $\geq inf_{\text{thresh}}$ **then**
        $s_i = s_j = I$
      end if
    end for
  end for
  for $i \in [1, N] \cap \mathbb{Z}$ **do**
    if $s_i = I \wedge Pois(\lambda_{rec}) \geq rec_{\text{thresh}}$ **then**
      $s_i = R$
    end if
  end for
  $\text{Res}_{t,1} \leftarrow \sum_{i=1}^{N} I[s_i = S]$
  $\text{Res}_{t,2} \leftarrow \sum_{i=1}^{N} I[s_i = I]$
  $\text{Res}_{t,3} \leftarrow \sum_{i=1}^{N} I[s_i = R]$
  $t \leftarrow t + 1$
end while
return Res

Algorithm 2 Simulation for Basic SIRV Model

Require: $S_t + I_t + R_t = N \; \forall t \wedge N, T \in \mathbb{Z}_+$

$x_1, x_2, ..., x_N \sim \mathcal{U}(\text{xmin}, \text{xmax}); y_1, y_2, ..., y_N \sim \mathcal{U}(\text{ymin}, \text{ymax})$

$$s_1, s_2, ..., s_N := \begin{cases} S & 1 \leq i \leq S_{t=0} \\ I & S_{t=0} < i \leq S_{t=0} + I_{t=0} \\ R & S_{t=0} + I_{t=0} \leq i \leq S_{t=0} + I_{t=0} + R_{t=0} \\ V & \text{otherwise} \end{cases}$$

Res $\leftarrow [0]^{N \times 4}$
t $= 1$
while $t \leq T$ **do**
  $m_1, m_2, ..., m_N \sim Bern(p_{\text{move}})$
  for $i = 1, i \leq N$ **do**
    if m_i **then**
      $x_i \leftarrow x_i + \mathcal{N}(0, 1)$
      $y_i \leftarrow y_i + \mathcal{N}(0, 1)$
    end if
  end for
  D $\leftarrow [0]^{N \times N}$
  for $i \in [1, N] \cap \mathbb{Z}$ **do**
    for $j \in [1, N] \cap \mathbb{Z}$ **do**
      $D_{i,j} = \sqrt{(x_i - x_j)^2 + (y_i - y_j)^2}$
    end for
  end for
  for $i \in [1, N] \cap \mathbb{Z}$ **do**
    for $j \in [i + 1, N] \cap \mathbb{Z}$ **do**
      if $(s_i = I \vee s_j = I) \wedge D_{i,j} < d_{\text{thresh}}$ **then**
        $\lambda_{inf} = |D_{i,j} - d_{\text{thresh}}|$
      end if
      infect $\leftarrow Pois(\lambda_{inf})$
      if permanent immunity **then**
        infect $\leftarrow 0$
      else if $s_i = R \vee s_j = R$ **then**
        infect $\leftarrow Pois(r_{inf} \cdot \lambda_{inf})$
      else if $s_i = V \vee s_j = V$ **then**
        infect $\leftarrow Pois(r_{\text{inf},V} \cdot \lambda_{inf})$
      end if
      if infect $\geq inf_{\text{thresh}}$ **then**
        $s_i = s_j = I$
      end if
    end for
  end for
  for $i \in [1, N] \cap \mathbb{Z}$ **do**
    if $s_i = I \wedge Pois(\lambda_{rec}) \geq rec_{\text{thresh}}$ **then**
      $s_i = R$
    else if $s_i = I \wedge Pois(\lambda_{vac}) \geq vac_{\text{thresh}}$ **then**
      $s_i = V$
    end if
  end for
  $\text{Res}_{t,1} \leftarrow \sum_{i=1}^{N} I[s_i = S]$
  $\text{Res}_{t,2} \leftarrow \sum_{i=1}^{N} I[s_i = I]$
  $\text{Res}_{t,3} \leftarrow \sum_{i=1}^{N} I[s_i = R]$
  $\text{Res}_{t,4} \leftarrow \sum_{i=1}^{N} I[s_i = V]$
  $t \leftarrow t + 1$
end while
return Res